communications earth & environment

ARTICLE

https://doi.org/10.1038/s43247-021-00280-x OPEN

Glacial lake outburst floods enhance benthic microbial productivity in perennially ice-covered Lake Untersee (East Antarctica)

Benoit Faucher[1✉], Denis Lacelle[1], Nicole Britney Marsh[2], Liam Jasperse[2], Ian Douglas Clark[2] & Dale Thomas Andersen[3]

Benthic ecosystems of perennially ice-covered lakes in Antarctica are highly sensitive to climate-driven changes. Lake Untersee has been in hydrological steady-state for several hundred years with a high pH water column and extremely low levels of dissolved inorganic carbon. Here, we show that glacial lake outburst floods can replenish carbon dioxide-depleted lakes with carbon, enhancing phototrophic activity of the benthic ecosystem. In 2019, a glacial lake outburst flood brought 17.5 million m^3 of water to Lake Untersee, the most substantial reported increase for any surface lake in Antarctica. High-resolution grain-size and carbon isotope analyses of microbial mats suggest that glacial lake outburst floods have occurred periodically over the Holocene and help explain the complex patterns of carbon cycling and sequestration observed in the lake. Our findings suggest that periodic flooding events may provide biological stimuli to other carbon dioxide-depleted Antarctic ecosystems and perhaps even icy lakes on early Mars.

[1] Department of Geography, Environment and Geomatics, University of Ottawa, Ottawa, Canada. [2] Department of Earth and Environmental Sciences, University of Ottawa, Ottawa, Canada. [3] Carl Sagan Center, SETI Institute, Mountain View, CA, USA. ✉email: bfaucher@uottawa.ca

Perennially ice-covered lakes are found in many regions of Antarctica, such as the McMurdo Dry Valleys (MDV), Bunger Hills, Vestfold Hills, Larsemann Hills, Schirmacher Oasis, and the Sôya Coast[1–3]. The majority of these lakes develop moats during the austral summer and are typically recharged annually by glacial meltwater that transports dissolved inorganic and organic carbon (DIC, DOC), cations and anions, nutrients, and sometimes other allochthonous materials[4,5]. Fluctuations in thaw-degree days in the upper catchment drive the production of meltwater influx thereby affecting the lake water levels[4]. For example, the summer of 2001–2002 in the MDV was exceptionally warm, and led to a glacial meltwater-sourced flooding of the lakes in Taylor Valley increasing their water level by 0.54–1.01 m[4,6].

Lake levels in glacial regions can also be influenced by glacial lake outburst floods (GLOFs): the sudden drainage of ice-marginal, ice-dammed or subglacial lakes[7,8]. GLOFs are typically reported from Iceland and Greenland, where the high discharge (mega-GLOF > 10^6 m^3) causes substantial damage to infrastructure and nearby communities[9]. Smaller magnitude GLOFs are also often reported from the Himalayas[10,11] and Andean Patagonian lakes and fjord[12,13]. However, GLOFs in Antarctica have been rarely reported. The only descriptions have been of a small GLOF in the Larsemann Hills (76,320 m^3) between 2017 and 2019, where ice-dammed lakes drained near the Russian Progress station[14], and the catastrophic drainage of a surface meltwater lake (600–750 million m^3) on the Amery Ice Shelf to the ocean below in East Antarctica in 2019[8]. However, the potential impacts of GLOFs on water chemistry and productivity of benthic microbial ecosystems in Antarctic ice-covered lakes remain unknown. Here, we provide evidence from Lake Untersee, a large ultra-oligotrophic perennially ice-covered lake in Dronning Maud Land (East Antarctica), that GLOFs can replenish the water column with dissolved carbon dioxide (CO_2) to help sustain the long-term primary production of benthic phototrophic communities.

Lake Untersee is located within the Untersee Oasis in the Gruber Mountains, c. 150 km south of the Princess Astrid Coast (Fig. 1). The local geology consists of plagioclase of the Precambrian Eliseev anorthosite-norite complex[2]. The Oasis contains two large perennially ice-covered lakes: Untersee and Obersee[15]. Lake Untersee is a 6.5 km long and 2.5 km wide ice-dammed lake (volume of 5.21×10^8 m^3) adjacent to the Anuchin Glacier and reaches a maximum depth of 169 m. A sill that cuts across the lake at 50 m depth separates the deeper northern basin from a smaller 100 m deep basin to the south. The North basin is nearly homo-thermal, well-oxygenated to the bottom, and well-mixed due to buoyancy-driven convection caused by melting of the ice-wall at the glacier-lake interface[16,17]. In contrast, the southern basin is density stratified below the sill depth and is anoxic at its bottom; the higher density prevents mixing with the overlying oxic water column[16,18,19]. Except for a large boulder field at the south end of the lake and a few other boulders scattered across the ice cover (n ~ 350 and most of them greater than 2 × 2 m), the surface of the ice cover on Lake Untersee is smooth and free of any fine sediments. The presence of the boulders is evidence for the presence of a thick, continuous ice cover for at least the past hundred years or perhaps throughout the Holocene[20]. The lake is recharged entirely by subaqueous melting of glacial ice and subglacial meltwater[21], and it has a Na(Ca)-SO_4 geochemical facies with high pH (10.6) that reflects a heritage of recharge from glacial meltwater, with minor contribution of Ca^{2+}-Na^+ solutes from in situ weathering of plagioclase and aluminosilicate minerals[22]. The total inorganic carbon (TIC) and total organic carbon (TOC) concentrations in the lake are very low (0.3–0.4 mg C L^{-1})[22], 1–3 orders of magnitude lower than in the MDV lakes and Antarctic subglacial lakes[23–26]. Despite the ultra-oligotrophic, low-light conditions, and lack of a seasonal moat, the lake hosts a benthic microbial ecosystem composed of photosynthetic microbial mats, small cuspate pinnacles, and large conical stromatolitic structures to depths of at least 130 m[27–30] (Fig. 2). The top layer of the microbial mats comprises a carbon-fixing cyanobacteria community (*Tychonema sp., Phormidium sp., Leptolyngbya sp*., and *Pseudanabaena sp*) that shift to a heterotrophic community in the underlying layers (*Actinobacteria, Verrucomicrobia, Proteobacteria*, and *Bacteroidetes*)[28,30,31]. The phototrophic mats are growing in very low light conditions: c. 5% of incident photosynthetically active radiation (PAR) irradiance is transmitted through the lake ice and decreases to c. 0.1% at a 135 m depth[27]. The benthic microbial mats were sampled by a scientific diver using 5 cm diameter core tubes at depths of 13, 17, and 18.5 m for subsequent analysis of organic C content, $\delta^{13}C_{org}$, and ^{14}C[22]. The organic C abundance of the mats ranged from 1.0 to 5.8 wt%, with the organic carbon density calculated at 793 ± 264 g m^{-2}. Despite showing some age reversals, the ^{14}C age distribution in the mats suggests that they are slowly accumulating biomass at a rate of c. 2.5 mm per 100 years. Carbon isotope analyses show that the cyanobacteria in the top 1 mm layer of the mats are fixing carbon without the isotopic fractionation of bicarbonate (HCO_3^-) from the high pH water or the respired CO_2 from heterotrophs in the layers of the underlying mat. As a result, it was inferred that the phototrophs growing in the upper-most layer of the mats are CO_2-depleted[22], resulting in lower gross photosynthesis and sequestration rates of organic carbon than the microbial mats in MDV lakes[29].

Lake Obersee is a smaller ice-dammed lake (volume of 8.07×10^7 m^3) located c. 6 km north-east of Untersee with a maximum depth of 83 m[31]. Like Untersee, Lake Obersee has a well-sealed ice cover with high pH (10–10.6) water and conductivity between 85 and 93 μS/cm^{-1}. The lake's water column has higher levels of dissolved nutrients and greater primary productivity than Untersee[32].

Lake Untersee, among the largest lakes in East Antarctica, is a closed-basin lake that remains tightly sealed from the atmosphere with no open water along the margin that would enhance gas exchange[33,34]. Despite a relatively warm mean annual air temperature (−9.5 ± 0.7 °C) and thawing degree-days (ranging from 7 to 51)[21,33], no surface streams have been observed entering the lake since work began there in 1969 due to the high ablation rate that limits surface melt of the Anuchin Glacier, as a result of cooling associated with the latent heat of sublimation[33,35]. Further, unlike lakes in the MDV and other regions in Antarctica, the water level of Lake Untersee has been stable for the past several decades[15,36], and based on the δD-$\delta^{18}O$ composition of the water column, the lake was likely in hydrological steady-state with no summer moating for at least the past 300–500 years[34]. However, during our field campaign in November–December 2019, we observed that the lake water level had increased by c. 2 m. This study aims to: (1) explain the cause of the increase in water level in Lake Untersee; and (2) examine the impact the large influx of water had on the lake chemistry and the benthic microbial ecosystem. These goals were achieved by: (1) reporting changes in lake level since 2004 using ICESat altimetry data; (2) determining changes in lake water chemistry (pH, major ions, δD-$\delta^{18}O$, TIC, TOC, and $\delta^{13}C_{TIC}$ and $^{14}C_{TIC}$); and (3) determining the amount of carbon stored in the lake to evaluate the effect of the large influx of water on the sustainability of the benthic ecosystem. This study provides important insight regarding the fate of this lake and other Antarctic lacustrine ecosystems impacted by the response of glaciers to a warming climate.

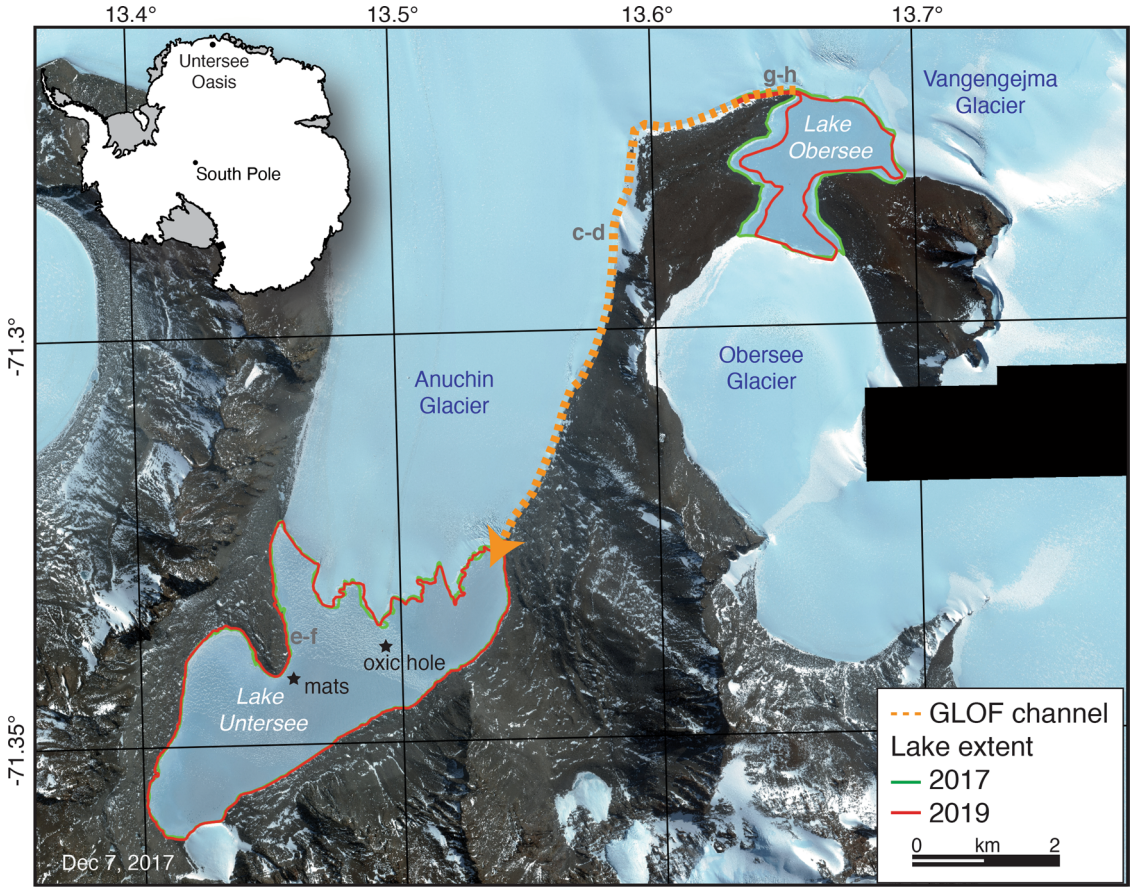

Fig. 1 Lake Untersee Oasis, Dronning Maud Land, Antarctica. Location map showing 2017–2019 extents of Lake Untersee and Lake Obersee and flow direction of the 2019 glacial lake outburst flood. Background Digital Globe NextView satellite imagery, December 7th, 2017; ©2020 Digital Globe NextView License (provided by NGA commercial imagery program). Map generated using QGIS 3.14. Letters indicate the location where photographs shown in Fig. 5 were taken. Stars indicate the sampling location of the benthic mats sampled in study[22] and the oxic water column.

Results and discussion

Description of the 2019 GLOF at Lake Untersee. ICESat-1 and ICESat-2 laser altimetry data show that the water levels of Lake Untersee and Lake Obersee remained stable between October 22nd, 2003 (the first acquisition date of ICESat-1 data) and mid-December 2018 (Fig. 3). However, the laser altimetry data indicates that the water level of Lake Untersee increased by 2.0 m between December 12th, 2018 and February 7th, 2019 (Fig. 3), and images from the time-lapse digital camera installed on our meteorological station revealed the sudden release of water through the ice cover on Jan 14–15th, 2019 (Fig. 4). Between the same dates, the water level of Lake Obersee decreased by 11.3 m. Therefore, the partial drainage of Lake Obersee caused the increase in water level at Lake Untersee. The sudden release of water from the North-West sector of Lake Obersee flowed for 8.3 km through a narrow channel along the east lateral moraine into the North-East corner of Lake Untersee. It resulted in the thermal erosion of the Anuchin Glacier and erosion of the east lateral moraine (Fig. 5). The inflow of GLOF waters also generated a 50 m wide melt pool in the North-East corner of Lake Untersee. Overall, the GLOF added 1.75×10^7 m^3 of water to Lake Untersee (a 3% increase in volume), whereas Lake Obersee experienced a decrease in volume of 2.29×10^7 m^3. Therefore, up to 25% of the water released from the GLOF may have also drained towards the coast. Since the GLOF in mid-January 2019, the water level of Lake Untersee has remained stable, whereas Lake Obersee is progressively infilling at a rate of 0.9 m $year^{-1}$ (Fig. 3).

Cause and magnitude of the GLOF. The ice flowing around Untersee Oasis is heavily disturbed by local mountains and nunataks, with glaciers flowing in different directions (the Anuchin Glacier represents a counter-current flow to the north flowing East Antarctic Ice Sheet). The partial drainage of Lake Obersee that caused the mid-January 2019 GLOF in Lake Untersee was likely due to a section of the Vangengejm Glacier that collapsed or shifted through a glacial tunnel, or by fast-moving ice-streams surrounding the Untersee Oasis (Fig. 5). The GLOF cannot be attributed to a surge or extensive surface melting of the Anuchin Glacier because the snout remained at the same location (Fig. 1). Further, the austral summer of 2018–2019 was not abnormally warm: the number of thawing degree days only reached 26.8 (ranking 6 out of 11 years). In fact, the water level of Lake Untersee has not been affected by annual fluctuations in thawing degree days (Fig. 3). Even at the maximum thawing degree days of 51, no surface melt was observed on the Anuchin Glacier due to the high ablation rate[21]. This contrasts with the lakes in the MDV, where water levels positively correlate with thawing degree days in the upper catchment area with increased contribution of glacial meltwater recharging the lakes.

The mid-January 2019 GLOF of Lake Untersee caused the most substantial single event increase in water level and volume of water for any surface lakes in Antarctica reported to date. In the MDV, a 1 m increase in water-level has a 100-years recurrence interval[4]. The 2017 and 2019 GLOFs at Larsemann Hills caused the water level of four lakes to increase by 0.4–1.5 m, which increased the water volume by a maximum of 76,320 m^3[14]. The GLOF at Lake Untersee

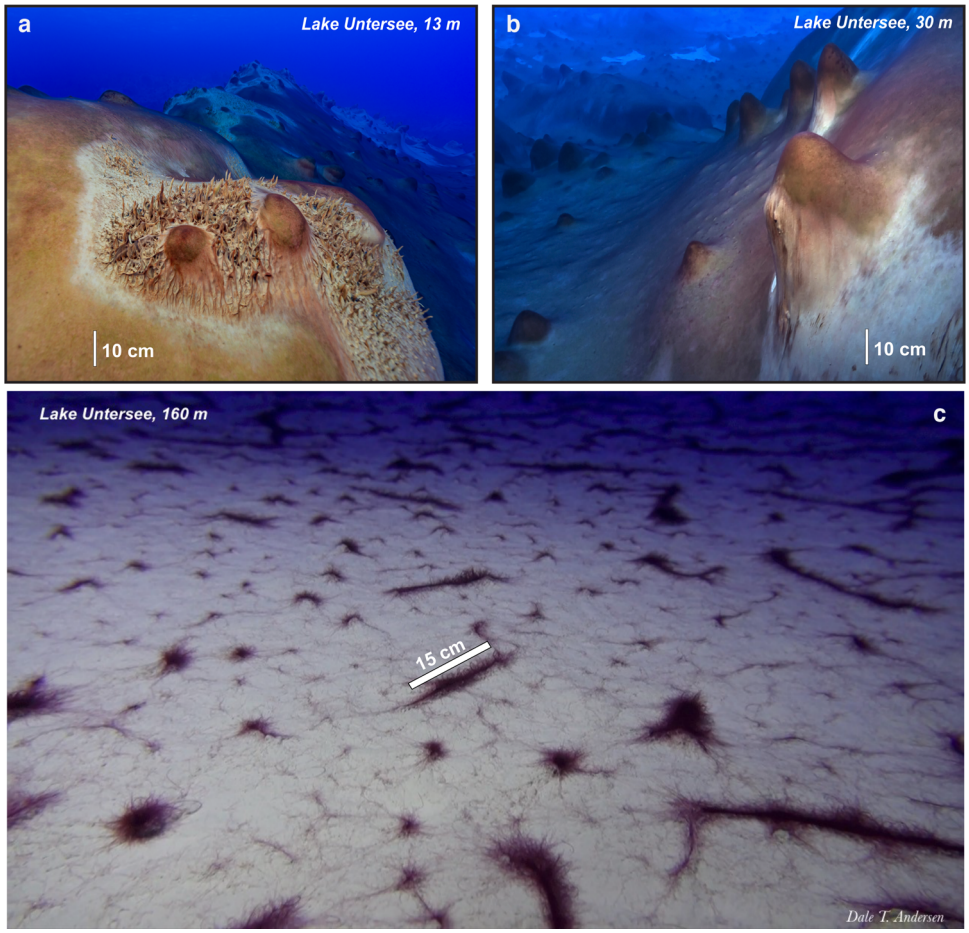

Fig. 2 Benthic microbial ecosystem in Lake Untersee, Antarctica. Photographs of laminated microbial mats, cones and pinnacles growing in Lake Untersee. **a**, **b** Photos of mats at 12–13 m and c. 30 m depth near the sampling location of mats. **c** Photo of mats at 160 m depth. Note the water column's clarity, reflecting the nutrient-starved water—photos taken by co-author D. Andersen.

increased the water level by 2 m over 21 days and added 1.75×10^7 m^3 of water to the lake (three orders of magnitude higher than the Larsemann Hills GLOF). We estimated the average discharge of the 2019 GLOF at ~ 9–10 $m^3\,s^{-1}$ (calculated from the increase in volume of water over 21 days), which is substantially lower than discharge rates associated with megafloods (>10^6 $m^3\,s^{-1}$) or catastrophic flooding events (>10^5 $m^3\,s^{-1}$) documented in Iceland[37–39]. Further, in terms of total flood volume, the 2019 Untersee GLOF was much lower than typical Icelandic jökulhlaups[7]. However, it was in the same range as some jökulhlaups recently inventoried in Greenland[40,41]. Therefore, despite having a relatively low estimated average discharge, the 2019 GLOF contributed a substantial volume of water to Lake Untersee that was sufficient to affect the chemical composition of the water column.

GLOF and its impacts on water chemistry. The mid-January 2019th GLOF altered the chemistry of the oxic water column of Lake Untersee from its stable composition that we have periodically measured since 2011, and that has remained unchanged since the early 1980s (Supplementary Table 1). The GLOF caused the pH to decrease from 10.5 to 9.5, specific conductivity decreased from 505–520 to 485 µS/cm^{-1}, and D.O. decreased from 150 to 128% (Fig. 3). The $\delta^{18}O$ composition showed little change (from -37.8 ± 0.3 to -37.4 ± 0.5‰), but the δD-$\delta^{18}O$ shifted from being distributed above the local meteoric water line (LMWL) to now plotting below it (D-excess decreased from 14.1 ± 0.7 to 7.9 ± 2.6‰). The TIC increased from 0.35 ± 0.05 mg C L^{-1} to 0.5 ± 0.02 mg C L^{-1} with $\delta^{13}C_{TIC}$ values decreasing from -9.1 ± 0.4‰ to -14.5 ± 1.9‰ and the $F^{14}C_{TIC}$ increasing from 0.4233 ± 0.02 to 0.5107–0.5481 (Fig. 3). The water that entered the lake in mid-January 2019 was not sampled because our field campaign ended in mid-December 2018. However, when we returned in late November 2019, a small stream was still flowing in the GLOF channel into the North-East corner of Lake Untersee; this stream had pH = 7.7, conductivity = 70 µS/cm^{-1}, $\delta^{18}O = -34.5$‰, D-excess = 3.2‰, TIC = 1.8 mg C L^{-1}, $\delta^{13}C_{TIC} = -18.5$‰, and $F^{14}C_{TIC} = 0.5844$.

The geochemical composition of the stream, assuming it originates from Lake Obersee, is very different from the high pH, low conductivity of Lake Obersee. Geochemical modeling using the *PHREEQC* hydrogeochemical software[42] suggests that the geochemical composition of the stream can be obtained following the drainage of Lake Obersee's water, and the weathering of plagioclase and biotite-bearing gneisses morainic material in equilibrium with atmospheric CO_2 as the water flows along the 8 km channel into Lake Untersee (Supplementary Table 2). Considering that the GLOF contributed 3%vol of water to Lake Untersee, a two-component mixing of the stream water chemistry being added to the lake matches reasonably well the post-GLOF conductivity and $\delta^{18}O$ values of the lake (Supplementary Table 3). However, parameters affected by exchanges with atmospheric gases, such as D.O., TIC, and $F^{14}C_{TIC}$, have mixing values that differ from those measured in the lake, which suggests additional interaction with the atmosphere. The lower D.O. is attributed to partial degassing of the water column of Lake Untersee through

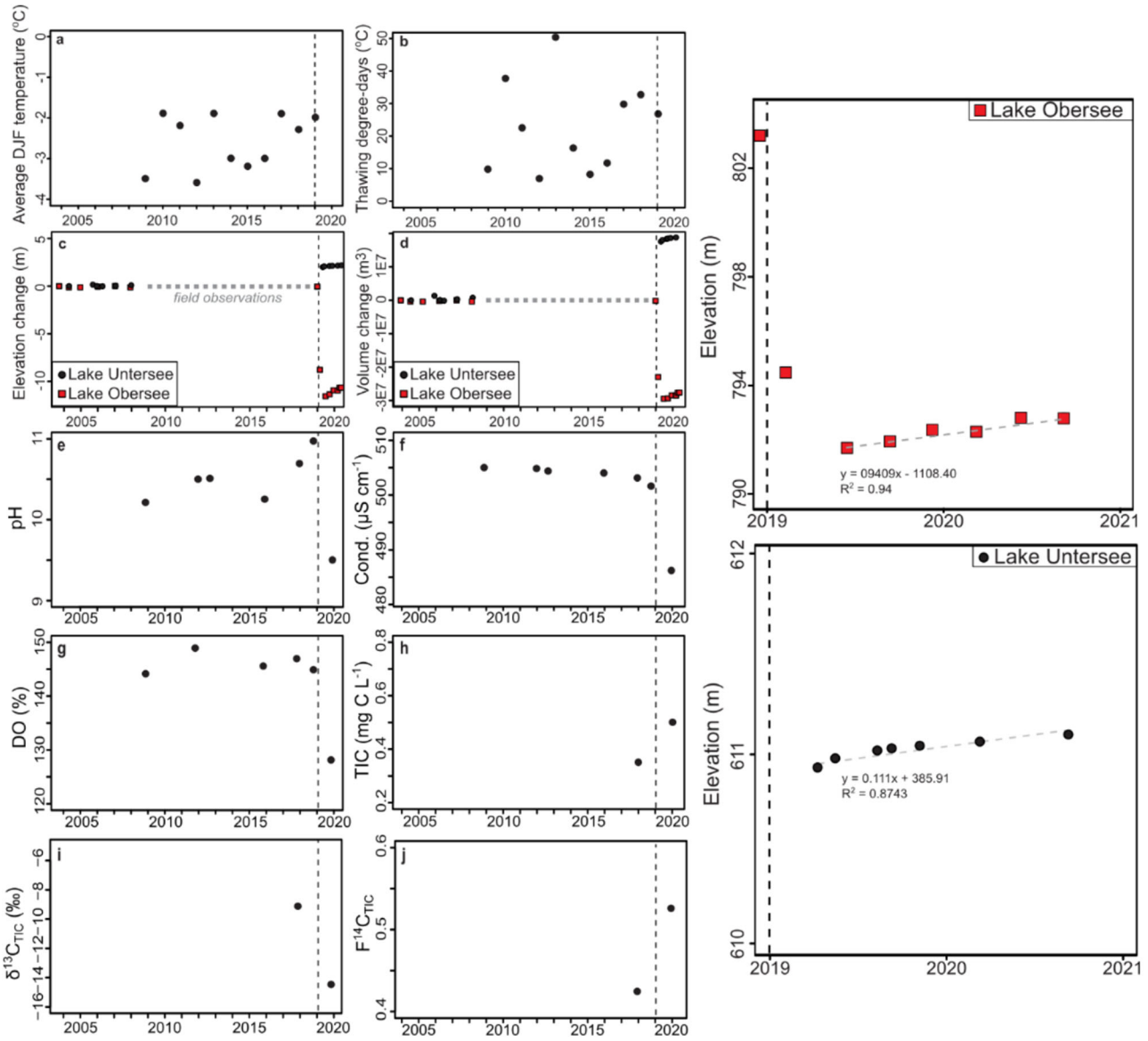

Fig. 3 2004–2020 Variations in hydrochemical parameters of Lake Untersee, Antarctica. a Average summer (December, January, and February; DJF) air temperature (°C) at Lake Untersee. **b** Thawing degree days at Lake Untersee (°C). **c**, **d** Changes in elevation (m) and volume (m^3) for lakes Untersee and Obersee (elevation data from ICESat and ICESat-2). **e–j** Mean values of pH, conductivity (µS/cm^{-1}), dissolved oxygen (DO%), total inorganic carbon (TIC; mg C L^{-1}), $\delta^{13}C_{TIC}$ (‰), and $F^{14}C_{TIC}$ in the oxic water column of Lake Untersee. The dashed vertical line represents the timing of the 2019 glacial lake outburst flood. The scatter plots on the right side of the figure show elevation (m) data for Lake Untersee and Lake Obersee after the 2019 GLOF event.

the c. 50 m wide moat that formed just beyond the stream entering the lake, or along fractures in the ice cover that developed from the rapid rise in water level. The higher TIC and $F^{14}C_{TIC}$ in the water column of the lake are attributed to additional uptake of modern atmospheric CO_2 from the small moat region. In fact, an additional uptake of 0.11 mg C L^{-1} (or 21%) of modern atmospheric CO_2 (with $F^{14}C = 1$) through the melt pool would be required to match both the measured post-GLOF TIC and $F^{14}C_{TIC}$. Satellite imagery indicated the small ice-free moat remained open until March 2019. Upon our return in November 2019, the ice cover in that area was more than 2 m thick.

Carbon stock and carbon mass balance of Lake Untersee. Based on the 2017 TIC–TOC measurements in the oxic water column and organic carbon content in microbial mats, Lake Untersee stores 5.42 to 6.71×10^9 g C, with >95% of the carbon pool residing in the microbial mats (Table 1). The TIC and TOC pools in the lake waters are 1.81×10^8 g C and 6.19×10^7 g C, respectively, with the organic C reservoir in the microbial mats reaching 5.17 to 6.47×10^9 g C. The latter was calculated from the average organic C content (793 ± 264 g m^2) of three cores collected near the push moraine, the surface area of the oxic lake bottom (8.15 km^2) and scaling to the three scenarios of mat coverage along the oxic lake bed: 100, 90, and 80% mat coverage. On occasion, small carbonate spherules can be found within the mat layers; however, these are uncommon and excluded from the carbon reservoir.

A carbon mass balance approach was used to determine if the 5.42 to 6.71×10^9 g C stored in Lake Untersee is in equilibrium with the carbon inputs under its hydrological steady-state condition, or if GLOFs can contribute carbon to help enhance productivity and subsequent sequestration of organic carbon within the CO_2-

Fig. 4 Time-lapse photography of glacial lake outburst flood in Lake Untersee, Antarctica. Glacial lake outburst flood started on January 14th–15th 2019, evidenced by the sudden release of water through the ice cover, which continued for many weeks.

depleted microbial mats. The carbon mass balance builds on the water mass balance of Lake Untersee[21]:

$$\Delta S = I_{sa} + I_{sg} - O_s, \quad (1)$$

where ΔS is the change in the volume of water, I_{sa} and I_{sg} are the contribution from subaqueous melting of terminus ice (originating from the melting of the submerged Anuchin Glacier at the ice–lake water interface) and subglacial meltwater (or other sources), respectively, and O_s is the surface outflow (sublimation of the ice cover). Recharge from precipitation (P) and surface water (I_s) were ruled out because they do not contribute to the lake; direct precipitation does not contribute to the lake since it has been well-sealed for the past 300–500 years, and there is no evidence for the influx of surface water feeding the lake via melt streams. Therefore, Untersee is only recharged by subaqueous melting of the Anuchin Glacier and subglacial meltwater and annually loses 0.6–1.2% of its water through ablation of the ice. Using an energy mass balance, it was determined that the subaqueous meltwater contributes 40–45% of the annual recharge, and the subglacial meltwater accounts for the remaining 55–60%[21].

The carbon mass balance can be calculated as:

$$\Delta\text{carbon}(g\,C) = I_{saTIC} + I_{saTOC} + I_{sgTIC} + I_{sgTOC} - O_{sTIC} - O_{sTOC}, \quad (2)$$

where I_{sa} and I_{sg} are the annual inflows of subaqueous melting of the Anuchin glacier's terminus ($1.98–2.23 \times 10^6\ m^3$) and subglacial meltwater contributions ($2.68–2.92 \times 10^6\ m^3$), and O_s is outflow surface waters via ice cover ablation ($3.22–6.43 \times 10^6\ m^3$).

As an initial scenario, the input of carbon into Lake Untersee assumes the lake is well-sealed and in hydrological steady-state (Supplementary Table 4). Subaqueous melting of the Anuchin Glacier at the lake-glacier interface (I_{saTIC} and I_{saTOC}) releases occluded atmospheric CO_2 gas directly in the water column that contributes $0.0165\ mg\,C\,L^{-1}$ as TIC[22]. The TOC released by the Anuchin Glacier flowing over the crystalline bedrock is assumed to be similar to that measured in the Vostok ice core from the interior of the East Antarctic Ice Sheet ($0.03\ g\,C\,L^{-1}$)[43]. The oxidation of the TOC in the water column and the oxidation of methane originating from the anoxic waters are not a substantial contributors to the TIC pool because $\delta^{13}C_{TIC}$ averages -9.1 ± 0.4‰, similar to the $\delta^{13}C_{CO2}$ of occluded gases (-7.3 to -6.3‰)[44,45]. We assume that the TIC–TOC concentrations in the subglacial meltwater recharging Lake Untersee (I_{sgTIC} and I_{sgTOC}) are similar to those calculated for the subaqueous meltwater with little to no carbonate dissolution or oxidation of organic material. A major contribution from subglacial carbonate dissolution or oxidation of organic carbon in the Precambrian crystalline bedrock[46,47] was ruled out in a previous study[22], because these carbonates and organics would have $\delta^{13}C$ values near 0 and c. -25‰, respectively[48], and would be ^{14}C dead, which would result in a very different $\delta^{13}C_{TIC}$ and $F^{14}C_{TIC}$ in the

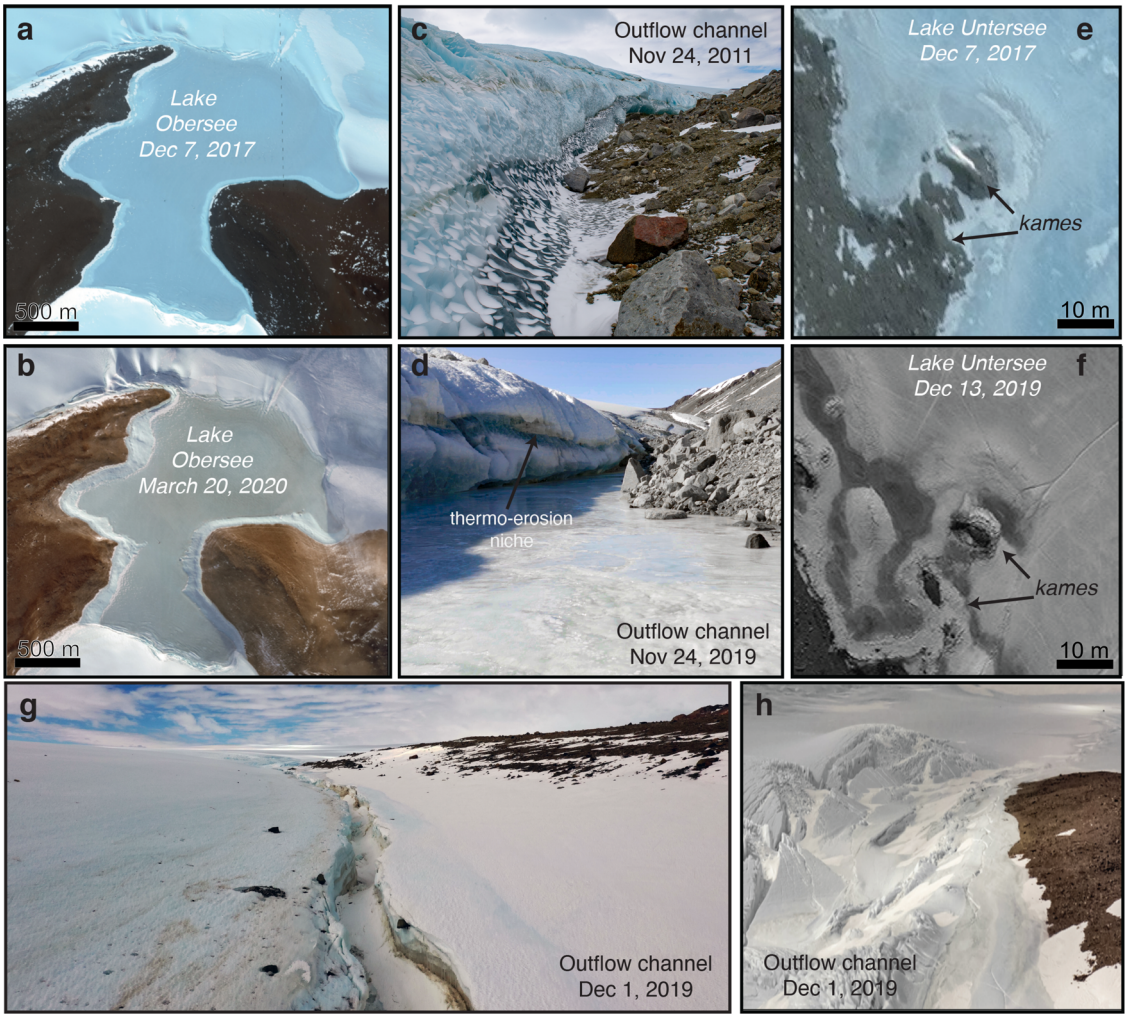

Fig. 5 Glacial lake outburst flood-related features in the Untersee Oasis. a Extent of Lake Obersee (December 7th, 2017). ©2020 Digital Globe NextView. **b** Extent of Lake Obersee (March 20th, 2020). ©2020 Digital Globe NextView. **c** Ancient outflow channel on the Anuchin Glacier's East lateral moraine (photo taken in Nov. 2011). The width of the reddish boulder in the central portion of the image is ~1 m. **d** thermally eroded outflow channel (~5 m in width) on the Anuchin Glacier's East lateral (photo taken in Nov. 2019). **e** Extent of ice coverage on two Kames on the North-East side of Lake Untersee's push moraine before the GLOF event (December 7th, 2017). ©2020 Digital Globe NextView. **f** Extent of ice coverage on two Kames on the North-East side of Lake Untersee's push moraine after the 2019 GLOF event (December 7th, 2017). ©2020 Digital Globe NextView. **g** Thermally eroded outflow channel (~4 m in width) at the North-East extremity of the Anuchin Glacier (image taken in Dec. 2019). **h** Outflow channel at the North-West extremity of Lake Obersee (photograph taken on December 5th, 2019). Width of the crevassed ice area is ~30 m.

Table 1 Amount of carbon stored in the oxic water column and microbial mats of Lake Untersee, Antarctica.

Reservoirs	Volume/surface area	Carbon (g C)
Lake oxic water	5.16E+08 m^3	2.43E+08
TIC (0.35 mg C L^{-1})		1.81E+08
TOC (0.12 mg C L^{-1})		6.19E+07
Mats		
S1 (1×)	8.15E+06 m^2	6.47E+09
S2 (0.9×)	7.34E+06 m^2	5.82E+09
S3 (0.8×)	6.52E+06 m^2	5.17E+09
Total		5.42–6.71E+09

The amount of carbon stored in mats was calculated using an organic carbon density of 793 ± 264 g m^2 and a surface area for the lake's oxic basin following three possible scenarios of mat coverage.
TIC total inorganic carbon, *TOC* total organic carbon.

water column and older ^{14}C age in the mats. In Lake Untersee, there is a minimal loss of carbon during the sublimation of ice cover (O_{sTIC}, O_{sTOC}): with the pH of the water column being 10.6, there is no CO_2 gas escaping through the sublimation of the ice cover (at pH 10.5, the DIC species are as bicarbonate and carbonate) and the soluble ions are segregated in the water column during freezing at the ice-water interface[49]. Therefore, taking the TIC and TOC concentrations of the subaqueous and subglacial meltwaters and their respective volume of water added annually, these two water sources would contribute 2.28×10^5 g C $year^{-1}$ (Supplementary Table 5). Lake Untersee formed 12–10 ka B.P., and assuming it remained well-sealed and in hydrological steady-state throughout its existence, our calculations are unable to account for all the carbon in the lake, and there must be other sources that contribute $3.11–4.21 \times 10^9$ g C (57–62% of the total carbon stock) (Fig. 6a).

The δD-$\delta^{18}O$ composition of Lake Untersee suggests that the lake has been well-sealed with no summer moating for the past 300–500 years[34]; however, a potential source for the missing carbon is the uptake of atmospheric CO_2 in the water column during a period when the lake possibly developed a summer moat along its margin. Paleo-temperature reconstructions show that the early Holocene in Dronning Maud Land was 1–2 °C warmer than today[50]. The warmer temperature caused the rapid thinning of the East Antarctic Ice Sheet[51], and the retreat of the glacier

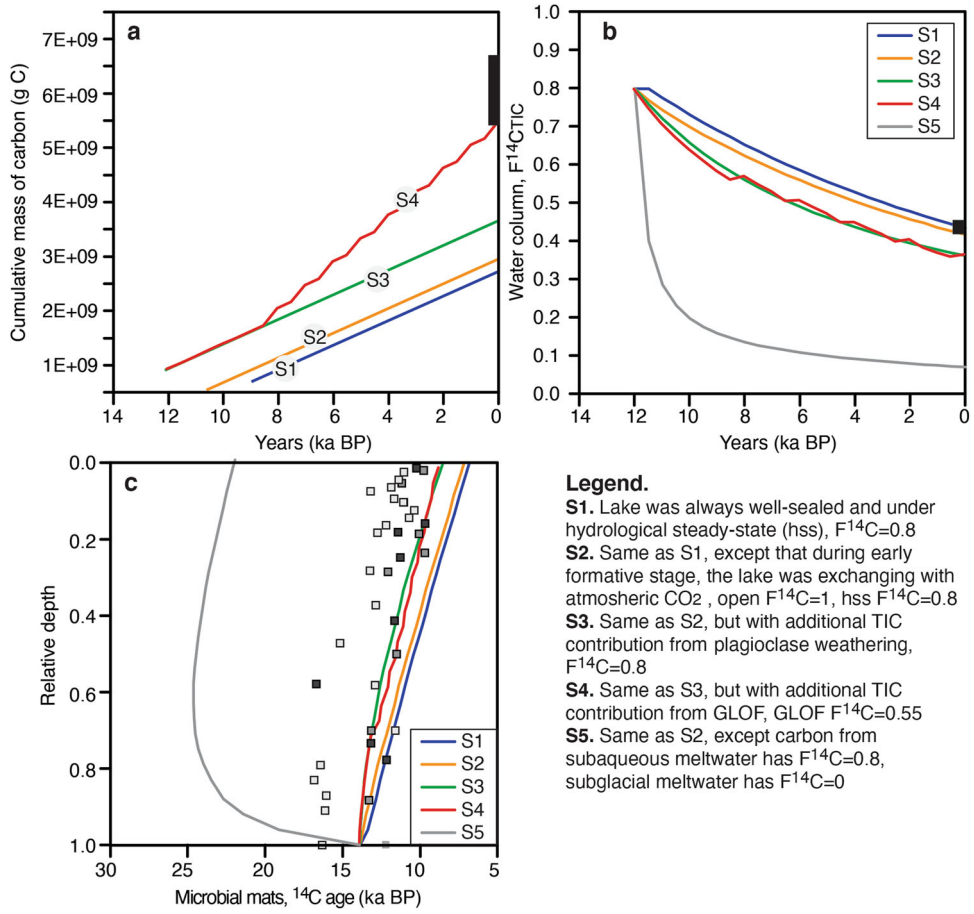

Fig. 6 Carbon mass balance and numerical modeling of ^{14}C evolution in the water column and microbial mats of Lake Untersee, Antarctica. a Cumulative mass of carbon (g C) accumulating in Lake Untersee's oxic water column and microbial mats under four different scenarios. Black bar is the amount of carbon stored in Lake Untersee. **b** Evolution of $F^{14}C_{TIC}$ in Lake Untersee under four different scenarios. Black bar is the measured $F^{14}C_{TIC}$ in the lake. **c** Evolution of ^{14}C age of microbial mats. The ^{14}C profile in the mats assumes the mats are solely using the TIC in lake water as their carbon source, and ^{14}C ages reflect the evolution of $^{14}C_{TIC}$ in the water column. White, black, and gray boxes, respectively indicate radiocarbon ages of microbial mat laminae in cores #1, #2, and #3.

from the valley subsequently filled the closed-basin valley and produced Lake Untersee[52]. During the early formative stage of Untersee, the lake likely developed a summer moat, as evidenced from the ^{14}C ages of bottom microbial mat layers (13–12 ka) that correspond to the timing of lake formation. This indicates that, at the time of lake formation, the cyanobacteria were fixing DIC under an open system with respect to CO_2 ($F^{14}C_{DIC} \sim 1$). Following cooling of regional air temperatures, the lake developed the tightly-sealed ice cover observed today. The water column likely became isolated from atmospheric CO_2 exchange shortly after 12 ka B.P., as indicated by the paucity of calcite observed in the mats[27]. The microbial mats consumed the DIC reservoir in the water column while continuing to receive DIC–DOC contributions from subaqueous and subglacial meltwaters. Therefore, assuming the water column was in equilibrium with the atmosphere during the early formative stage of Lake Untersee, geochemical modeling predicts that the weathering of plagioclase minerals from glacial meltwater would generate pH near 10.5 with DIC reaching 1.3–1.5 mg C L^{-1} (Supplementary Table 2). If the lake then became well-sealed shortly after it formed and was being recharged solely by the subaqueous and subglacial meltwaters, similar to hydrological conditions over the past few hundred years, carbon mass balance calculation indicates the lake would have accumulated 3.51×10^9 g C, which is still 3–3.6 $\times 10^9$ g C lower than the estimated total carbon reservoir (Fig. 6).

GLOFs and carbon mass balance of Lake Untersee. The 2019 GLOF added c. 1.75×10^7 m^3 of water to Lake Untersee and replenished the oxic water column of Lake Untersee with c. 1.40×10^8 g C (Supplementary Table 4). The amount of carbon added by this single GLOF event is, nevertheless, about an order of magnitude too low to explain the total carbon stored in Lake Untersee. However, high-resolution analyses in the microbial mat cores collected near the push moraine revealed individual matching layers with higher sand fraction, lower $\delta^{13}C_{org}$ values and higher $F^{14}C$ values (Fig. 7). We suggest that these shared characteristics in the mats are due to previous GLOFs contributing carbon and other nutrients to Lake Untersee.

Unlike ice-covered lakes in the MDV[53–55], the surface ice cover of Lake Untersee is free of any fine sediments, and the main source of sediments is glacial flour derived from subaqueous and subglacial meltwaters[27]. The 2019 GLOF, with an estimated discharge of 9–10 m^3 s^{-1}, had sufficient velocity to transport sand-sized sediments that would be deposited into the lake. Observations of a potential thin layer of sand on the mats' surface have yet to be made since the most recent samples in hand were collected in December 2017. Nonetheless, we did observe for the

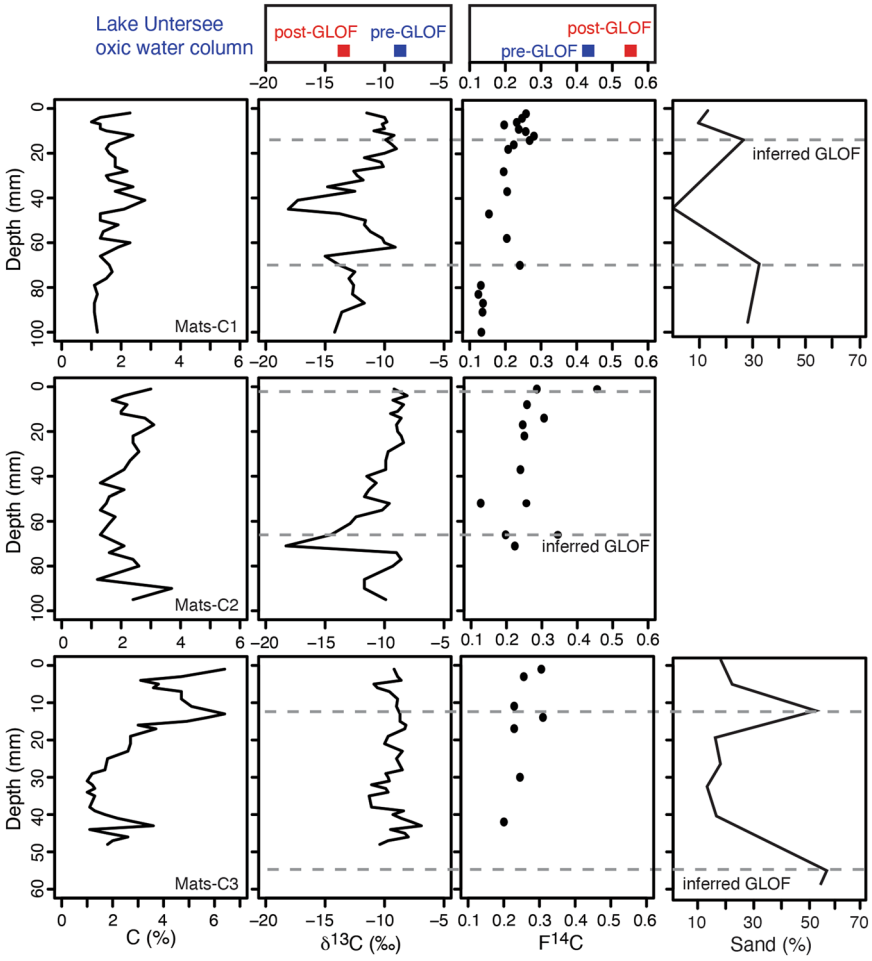

Fig. 7 Organic carbon content (C %), $\delta^{13}C$ (‰), $F^{14}C$, and sand-fraction (%) of three microbial mat cores sampled in Lake Untersee, Antarctica. Cores were collected in proximity to photographs shown in Fig. 2. Dashed lines associate increases in sand-size fraction (%) within the mats with increases in $F^{14}C$ and decreases in $\delta^{13}C$ (‰). These changes in particle size distribution and carbon isotopes in the mats are inferred to be related to GLOFs that transport sand and supply TIC into Lake Untersee with a lower $\delta^{13}C_{TIC}$ and higher $F^{14}C_{TIC}$ signature relative to the water column. Also shown for comparison are the $\delta^{13}C_{TIC}$ (‰) and $F^{14}C_{TIC}$ values in the water column of Lake Untersee before and after the 2019 GLOF.

first time a thin layer of fine sediment covering light sensors that we retrieved in December 2019. The 2019 GLOF also increased the TIC and $F^{14}C_{TIC}$ in the oxic water column and decreased the $\delta^{13}C_{TIC}$ (Fig. 3), characteristics also observed in the $\delta^{13}C$ and ^{14}C of some layers in the mats. After a GLOF of this magnitude, the cyanobacteria in the top mat layer would be fixing the HCO_3^- with this modified $\delta^{13}C_{TIC}$ and $F^{14}C_{TIC}$ signatures, and that would be recorded in the $\delta^{13}C_{org}$ and ^{14}C of the microbial mat since fixation of the HCO_3^- would likely still occur with no ^{13}C fractionation due to the high pH (9.5) and still relatively low TIC (0.5 ppm C)[22]. In fact, the mats show these concurrent shifts in $\delta^{13}C$ and $F^{14}C$ at distinct layers (sampled 1–2 mm layers which represent 50–100 years accumulation period). As the microbial mats progressively sequester the DIC reservoir in the water column, while continuing to receive DIC–DOC contribution from subaqueous and subglacial meltwaters with different $\delta^{13}C_{TIC}$ and $F^{14}C_{TIC}$ compositions relative to the GLOF, the $\delta^{13}C_{TIC}$ in the water column will, over time, evolve to those measured before the 2019 GLOF while the $F^{14}C_{TIC}$ will evolve following its decay. As a result, a shift in grain size and carbon isotopes within a single mat layer can be used as proxies of GLOF occurrences (Fig. 7). However, it should be noted that a change in grain size and carbon isotopes is unlikely to be identical in the mats throughout the 6.5 km long Lake Untersee due to limnological factors (e.g., water circulation, topography) and variations in metabolism and carbon assimilation within the mats due to differences in other stressors (i.e., light attenuation with depth, availability of other nutrients). A gradient in sediment deposition following a GLOF is expected with coarser material deposited in the North-East corner of the lake, where the GLOF entered the lake and fining of sediments with increasing distance. This is likely why only a thin layer of sand was observed in the mats sampled near the push moraine (3.5 km from the corner where the GLOF entered the lake). Thus, our results from the mats provide evidence that GLOFs sporadically recharged Lake Untersee over the Holocene, and the presence of multiple strandlines above Lake Untersee supports this assumption.

Assuming GLOFs of similar magnitude and chemical composition occurred on several occasions over the Holocene (at least five times), with the lake being recharged solely by subaqueous and subglacial meltwater during that period, we can explain the total carbon reservoir using the carbon balance calculation (Fig. 6a). In addition, numerical modeling of the evolution of $F^{14}C_{TIC}$ in the oxic water column and the ^{14}C age distribution in the microbial mats following the addition of younger carbon to the lake by the GLOF also agrees well with the measurements (Fig. 6b, c). Therefore, our findings demonstrate that GLOFs can contribute substantially to the long-term accumulation of biomass and overall productivity of CO_2-depleted perennially ice-covered lakes, such as Lake Untersee, by periodically

supplying them with carbon sources. Our findings contribute to the body of literature that GLOFs increase the productivity of lacustrine or fjord ecosystems. GLOFs were also found to be beneficial to phototrophs in Patagonian lakes, where floods decreased turbidity and increased light penetration due to a reduction in clays into the lake[13]. In the Northern Patagonian Ice Field, GLOFs increased terrestrial particulate organic carbon and populations of *Munida gregaria*, which connects organic carbon to the higher trophic levels[12].

Our findings also have relevance for the potential habitability of CO_2-depleted lakes on early Mars. As suggested by previous studies[56,57], well-sealed perennially ice-covered lakes in Antarctica provide relevant analogs that may help explain the lack of observed carbonates in the paleolacustrine sediments of Gale Crater (which was likely an ice-covered lake during the Hesperian[58]) despite a higher CO_2 level in the atmosphere during that early period of Martian history. As shown in Lake Untersee, with its CO_2-depleted water column, and sediments nearly carbonate-free, such lakes can still sustain robust benthic microbial communities. This light and CO_2-depleted aquatic environment provides a useful analog for assessing the habitability of other planetary bodies, and to inform and improve strategies for the search for life beyond Earth.

Methods

Changes in elevation and water volume for Lake Untersee and Lake Obersee. Surface elevation changes of lakes Untersee and Obersee during the 2004–2020 period were assessed using ICESat and ICESat-2 (ATL06 products) datasets available on the *Open Altimetry* web-based application[59,60]. ICESat and ICESat-2 altimetry data have vertical precisions of ~14 and 0.4 ± 2–4 cm, respectively[61,62]. Although the altimetry data represents elevation at discrete points, we assume in our temporal analysis that the elevation of the ice cover is constant across the surface of the lakes. Changes in lake water volume were subsequently determined from digitized, georeferenced bathymetric maps of Lake Untersee and Lake Obersee produced with measurements made during previous field seasons[18,63]; volume and surface area calculations were made with the *Surface Volume* tool in the *ArcGIS pro 2.4* software.

Lake water analyses. During the field season at Lake Untersee in November 2019, measurements of pH, temperature, specific conductivity, total dissolved solids (TDS), dissolved oxygen (DO), and chlorophyll were made using a calibrated Hydrolab DS5 Water Quality Sonde lowered through 25 cm holes drilled in the ice cover within the North and South basins (Fig. 1). Lake water samples were collected at 5–10 m intervals from the same locations of previous years using a clean 2.5 L Niskin bottle. The water samples were immediately transferred into sampling bottles unfiltered due to the ultra-clear and low-particulate content in the waters, and the sensitivity of the high pH waters to the rapid absorption of atmospheric CO_2 that would affect pH and dissolved inorganic carbon (DIC)[22]. Water samples for TIC-TOC analyses were collected in 40 mL amber glass vials with butyl septa caps. Radiocarbon samples were collected in pre-baked (500 °C for 3 h) 1 L amber glass amber bottles.

The TIC–TOC concentration and stable isotope ratios ($\delta^{13}C_{TIC}$, $\delta^{13}C_{TOC}$) in lake waters were measured by a wet TOC analyzer interfaced with a Thermo DeltaPlus XP isotope-ratio mass spectrometer at the Ján Veizer Stable Isotope Laboratory (University Ottawa) using methods described in this study[64]. The isotope ratios are presented as per mil deviation relative to VPDB and expressed using the delta-notation. The 2σ analytical precision is ±0.5 ppm for TIC and TOC concentrations and ±0.2‰ for $\delta^{13}C_{TIC}$ and $\delta^{13}C_{TOC}$.

Radiocarbon analysis of TIC-TOC in waters was performed at the A.E. Lalonde Accelerator Mass Spectrometry Laboratory, University of Ottawa. Sample preparation, extraction of inorganic and organic carbon from waters and graphitization were performed according to this study[65]. Graphitized samples were analyzed on a 3MV tandem mass spectrometer. The $^{14}C/^{12}C$ ratios are expressed as fraction of modern carbon ($F^{14}C$) and corrected for spectrometer and preparation fractionation using the AMS measured $^{13}C/^{12}C$ ratio[66,67]. Radiocarbon ages are calculated as $-8033\ln(F^{14}C)$ and are reported in ^{14}C year B.P. (BP = AD1950)[68]. The 2σ errors are reported with the results and <0.013 $F^{14}C$ (or <190 years).

Carbon mass balance. A carbon mass balance approach was used to assess if the amount of organic carbon stored in the microbial mats and the oxic water column of Lake Untersee is in equilibrium with carbon inputs into the lake. The carbon stored in the mats was calculated from the organic C content of three cores, the surface area of the oxic lake bottom (8.15 km^2) and scaling to the three scenarios of mat coverage along the oxic lake bed: 100, 90, and 80% mat coverage (data from this study[22]). The data for TIC–TOC, $\delta^{13}C_{TIC}$, and $F^{14}C_{TIC}$ in the oxic water before the mid-January 2019 GLOF is taken from Table 4 in this study[22] and determined using the methods described in the previous section.

Based on the annual inputs of carbon to the lake, the cumulative mass of carbon in the lake ecosystem, and the evolution of $F^{14}C_{TIC}$ in the oxic water column and ^{14}C in mats over the past 12 ka (since the formation of the lake) were calculated for four different scenarios and compared to our measurements (Supplementary Table 5): (S1) the lake was always well-sealed and under hydrological steady-state, as observed presently; (S2) during the early formative stage, the water column of the lake was exchanging with atmospheric CO_2 with no weathering, but then switched to a well-sealed ice cover and was under hydrological steady-state; (S3) same as S2, but with additional TIC contribution from open system weathering of plagioclase minerals; (S4) same as S3, but with additional TIC contribution from GLOFs. The cumulative mass of carbon was calculated in 500-year time-steps. The evolution of $F^{14}C_{TIC}$ follows the accumulation of carbon to the lake with $F^{14}C$ of 0.8 (estimated from the age of occluded CO_2 gases being released into the lake)[34] and its decay over time using the half-life = 5730 years. The ^{14}C profile in the mats assumes the mats are using the TIC solely in lake water as their carbon source, and ^{14}C mats reflect the evolution of $^{14}C_{TIC}$ in the water column. However, due to the substantial carbon reservoir effect in the water column, the ^{14}C ages of the mats cannot be calibrated to calendar years, and an age-depth model cannot be performed.

Data availability

The Lake Untersee water column and microbial mat biogeochemical data used in this study are available through the National Snow and Ice Data Center (nsidc.org). The ICESat-1 and ICESat-2 laser altimetry datasets used for this study are available at: https://openaltimetry.org/.

Received: 13 July 2021; Accepted: 14 September 2021;
Published online: 05 October 2021

References

1. Matsumoto, G. I. et al. Geochemical characteristics of Antarctic lakes and ponds. *Proc. NIPR Symp. Polar Biol.* **5**, 125–145 (1992).
2. Bormann, P. The Schirmacher Oasis, Queen Maud Land, East Antarctica and its surroundings. *Polarforschung* **64**, 151–153 (1995).
3. Perriss, S. J. & Laybourn-Parry, J. Microbial communities in saline lakes of the Vestfold hills (eastern Antarctica). *Polar Biol.* **18**, 135–144 (1997).
4. Doran, P. T. et al. Hydrologic response to extreme warm and cold summers in the McMurdo Dry Valleys, East Antarctica. *Antarct. Sci.* **20**, 499–509 (2008).
5. Tanabe, Y. et al. Abundant deposits of nutrients inside lakebeds of Antarctic oligotrophic lakes. *Polar Biol.* **40**, 603–613 (2017).
6. Gooseff, M. N. et al. Decadal ecosystem response to an anomalous melt season in a polar desert in Antarctica. *Nat. Ecol. Evol.* **1**, 1334–1338 (2017).
7. Carrivick, J. L. & Tweed, F. S. A review of glacier outburst floods in Iceland and Greenland with a megafloods perspective. *Earth Sci. Rev.* **196**, 102876 (2019).
8. Warner, R. C. et al. Rapid formation of an ice doline on Amery Ice Shelf, East Antarctica. *Geophys. Res. Lett.* https://doi.org/10.1029/2020gl091095 (2021).
9. Dubey, S. & Goyal, M. K. Glacial lake outburst flood hazard, downstream impact, and risk over the Indian Himalayas. *Water Resour. Res.* **56**, e2019WR026533 (2020).
10. Khadka, N. et al. Evaluation of glacial lake outburst flood susceptibility using multi-criteria assessment framework in Mahalangur Himalaya. *Front. Earth Sci.* **8**, 748 (2021).
11. Veh, G., Korup, O. & Walz, A. Hazard from Himalayan glacier lake outburst floods. *Proc. Natl. Acad. Sci.* **117**, 907 (2020).
12. Meerhoff, E., Castro, L. R., Tapia, F. J. & Pérez-Santos, I. Hydrographic and biological impacts of a glacial lake outburst flood (GLOF) in a Patagonian Fjord. *Estuar. Coasts* **42**, 132–143 (2019).
13. Bastidas Navarro, M., Martyniuk, N., Balseiro, E. & Modenutti, B. Effect of glacial lake outburst floods on the light climate in an Andean Patagonian lake: implications for planktonic phototrophs. *Hydrobiologia* https://doi.org/10.1007/s10750-016-3080-4 (2018).
14. Pryakhina, G. V., Boronina, A. S., Popov, S. V. & Chetverova, A. A. Hydrological studies of lake outbursts in the Antarctic Oases. *Russ. Meteorol. Hydrol.* **45**, 118–123 (2020).
15. Hermichen, W. D., Kowski, P. & Wand, U. Lake Untersee, a first isotope study of the largest freshwater lake in the interior of East Antarctica. *Nature* **315**, 131–133 (1985).
16. Wand, U., Schwarz, G., Brüggemann, E. & Bräuer, K. Evidence for physical and chemical stratification in Lake Untersee (central Dronning Maud Land, East Antarctica). *Antarct. Sci.* **9**, 43–45 (2007).

17. Steel, H. C. B., McKay, C. P. & Andersen, D. T. Modeling circulation and seasonal fluctuations in perennially ice-covered and ice-walled lake untersee, antarctica. *Limnol. Oceanogr.* **60**, 1139–1155 (2015).
18. Wand, U., Samarkin, V. A., Nitzsche, H.-M. & Hubberten, H.-W. Biogeochemistry of methane in the permanently ice-covered Lake Untersee, central Dronning Maud Land, East Antarctica. *Limnol. Oceanogr.* **51**, 1180–1194 (2006).
19. Bevington, J. et al. The thermal structure of the anoxic trough in Lake Untersee, Antarctica. *Antarct. Sci.* **30**, 333–344 (2018).
20. Wand, U. & Perlt, J. Glacial boulders 'floating' on the ice cover of Lake Untersee, East Antarctica. *Antarct. Sci.* **11**, 256–260 (2007).
21. Faucher, B., Lacelle, D., Fisher, D. A., Andersen, D. T. & McKay, C. P. Energy and water mass balance of lake Untersee and its perennial ice cover, East Antarctica. *Antarct. Sci.* **31**, 271–285 (2019).
22. Marsh, N. B. et al. Sources of solutes and carbon cycling in perennially ice-covered Lake Untersee, Antarctica. *Sci. Rep.* **10**, 1–12 (2020).
23. Lyons, W. B. et al. The carbon stable isotope biogeochemistry of streams, Taylor Valley, Antarctica. *Appl. Geochem.* **32**, 26–36 (2013).
24. Neumann, K., Lyons, W. B., Priscu, J. C., Desmarais, D. J. & Welch, K. A. The carbon isotopic composition of dissolved inorganic carbon in perennially ice-covered Antarctic lakes: searching for a biogenic signature. *Ann. Glaciol.* **39**, 518–524 (2004).
25. Takacs, C. D., Priscu, J. C. & McKnight, D. M. Bacterial dissolved organic carbon demand in McMurdo dry valley lakes, Antarctica. *Limnol. Oceanogr.* **46**, 1189–1194 (2001).
26. Vick-Majors, T. J. et al. Biogeochemical connectivity between freshwater ecosystems beneath the West Antarctic Ice Sheet and the sub-ice marine environment. *Glob. Biogeochem. Cycles* **34**, no–no (2020).
27. Andersen, D. T., Sumner, D. Y., Hawes, I., Webster-Brown, J. & Mckay, C. P. Discovery of large conical stromatolites in Lake Untersee, Antarctica. *Geobiology* **9**, 280–293 (2011).
28. Greco, C. et al. Microbial diversity of pinnacle and conical microbial mats in the perennially ice-covered lake Untersee, East Antarctica. *Front. Microbiol.* **11**, 1–16 (2020).
29. Hawes, I., Sumner, D. & Jungblut, A. D. in *The Structure and Function of Aquatic Microbial Communities. Advances in Environmental Microbiology*, vol 7. (ed. Hurst, C.) 91–120 (Springer, 2019).
30. Velichko, N., Smirnova, S., Averina, S. & Pinevich, A. A survey of Antarctic cyanobacteria. *Hydrobiologia* **848**, 2627–2652 (2021).
31. Koo, H. et al. Microbial communities and their predicted metabolic functions in growth laminae of a unique large conical mat from lake Untersee, East Antarctica. *Front. Microbiol.* **8**, 1–15 (2017).
32. Haendel, D. & Kaup, E. in *The Schirmacher Oasis, Queen Maud Land, East Antarctica, and its Surroundings* (eds Bormann, P. & Fritzshe, D.) (Justus Perthes Verlag, 1995).
33. Andersen, D. T., McKay, C. P. & Lagun, V. Climate conditions at perennially ice-covered lake Untersee, East Antarctica. *J. Appl. Meteorol. Climatol.* **54**, 1393–1412 (2015).
34. Faucher, B., Lacelle, D., Fisher, D. A., Weisleitner, K. & Andersen, D. T. Modeling δD-δ18O steady-state of well-sealed perennially ice-covered lakes and their recharge source: examples from Lake Untersee and lake Vostok, Antarctica. *Front. Earth Sci.* **8**, 220 (2020).
35. Hoffman, M. J., Fountain, A. G. & Liston, G. E. Surface energy balance and melt thresholds over 11 years at Taylor Glacier, Antarctica. *J. Geophys. Res. Earth Surf.* **113**, 1–12 (2008).
36. E. Kaup, A. Loopmann, V. Klokov, I. Simonov, D. H. in *Limnological Studies in Queen Maud Land* (East Antarctica) (ed. Martin, J.) 28–42 (Valgus, 1988).
37. Baker, V. R. In *Flood and Megaflood Processes and Deposits: Recent and Ancient Examples* (eds Martini, P. et al.) 3–15 (Blackwell, 2002).
38. Carling, P. A. Freshwater megaflood sedimentation: what can we learn about generic processes? *Earth Sci. Rev.* **125**, 87–113 (2013).
39. Björnsson, H. Understanding jökulhlaups: from tale to theory. *J. Glaciol.* **56**, 1002–1010 (2010).
40. Mayer, C. & Schuler, T. V. Breaching of an ice dam at Qorlortossup tasia, south Greenland. *Ann. Glaciol.* **42**, 297–302 (2005).
41. Higgins, A. K. On some ice-dammed lakes in Frederikshåb district, south-West Greenland. *Meddelelser fra Dansk Geol. Foren.* **19**, 378–397 (1970).
42. Parkhurst, D. L. & Appelo, C. A. J. Description of input and examples for PHREEQC Version 3—A Computer Program for speciation, batch-reaction, one-dimensional transport, and inverse geochemical calculations. *U.S. Geol. Surv. Tech. Methods* https://doi.org/10.1016/0029-6554(94)90020-5 (2013).
43. Lyons, W. B., Welch, K. A., Priscu, J. C., Tranter, M. & Royston-Bishop, G. Source of Lake Vostok cations constrained with strontium isotopes. *Front. Earth Sci.* **4**, 78 (2016).
44. Eggleston, S., Schmitt, J., Bereiter, B., Schneider, R. & Fischer, H. Evolution of the stable carbon isotope composition of atmospheric CO2 over the last glacial cycle. *Paleoceanography* **31**, 434–452 (2016).
45. Schmitt, J. et al. Carbon isotope constraints on the deglacial CO_2 rise from ice cores. *Science* https://doi.org/10.1126/science.1217161 (2012).
46. Wadham, J. L. et al. Biogeochemical weathering under ice: size matters. *Glob. Biogeochem. Cycles* **24**, 3 (2010).
47. Wynn, P. M., Hodson, A. & Heaton, T. Chemical and isotopic switching within the subglacial environment of a high Arctic Glacier. *Biogeochemistry* **78**, 173–193 (2006).
48. Clark, I. *Groundwater Geochemistry and Isotopes* (CRC Press, 2015).
49. Santibáñez, P. A., Michaud, A. B. & Majors, T. J. V. Differential incorporation of bacteria, organic matter, and inorganic ions into lake ice during iceformation. *J. Geophys. Res.* https://doi.org/10.1029/2018JG004825 (2019).
50. Ciais, P., Jouzel, J., Petit, J. R., Lipenkov, V. & White, J. W. C. Holocene temperature variations inferred from six Antarctic ice cores. *Ann. Glaciol.* **20**, 427–436 (1994).
51. Mackintosh, A. N. et al. Retreat history of the East Antarctic Ice Sheet since the last glacial maximum. *Quat. Sci. Rev.* **100**, 10–30 (2014).
52. Hiller, A., Wand, U., Kampf, H. & Stackebrandt, W. Occupation of the Antarctic continent by petrels during the past 35,000 years: inferences from a 14C study of stomach oil deposits. *Polar Biol.* **9**, 69–77 (1988).
53. Wharton, R. A. et al. Changes in ice cover thickness and lake level of Lake Hoare, Antarctica: implications for local climatic change. *J. Geophys. Res.* **97**, 3503–3513 (1992).
54. Jepsen, S. M., Adams, E. E. & Priscu, J. C. Sediment melt-migration dynamics in perennial antarctic lake ice. *Arctic Antarct. Alp. Res.* **42**, 57–66 (2010).
55. Squyres, S. W., Andersen, D., Nedell, S. S. & Wharton, R. A. Lake Hoare, Antarctica: sedimentation through a thick perennial ice cover. *Sedimentology* **38**, 363–379 (1991).
56. Fairén, A. Icy Mars lakes warmed by methane. *Nat. Geosci.* **10**, 717–718 (2017).
57. McKay, C. P., Andersen, D. & Davila, A. Antarctic environments as models of planetary habitats: University Valley as a model for modern Mars and Lake Untersee as a model for Enceladus and ancient Mars. *Polar J.* **7**, 303–318 (2017).
58. Kling, A. M., Haberle, R. M., McKay, C. P., Bristow, T. F. & Rivera-Hernandez, F. Subsistence of ice-covered lakes during the Hesperian at Gale crater, Mars. *Icarus* **338**, P.113495 (2020).
59. Nandigam, V. et al. Rapid access and visualization of spaceborne altimetry data from ICESAT and ICESAT-2. in *International Geoscience and Remote Sensing Symposium (IGARSS)* https://doi.org/10.1109/IGARSS.2018.8518105 (2018).
60. Smith, B. et al. ATLAS/ICESat-2 L3A land ice height, version 3. [ATL06]. NASA National Snow and Ice Data Center Distributed Active Archive Center. https://doi.org/10.5067/ATLAS/ATL06.003 (2020).
61. Brenner, A. C., DiMarzio, J. P. & Zwally, H. J. Precision and accuracy of satellite radar and laser altimeter data over the continental ice sheets. *IEEE Trans. Geosci. Remote Sens.* https://doi.org/10.1109/TGRS.2006.887172 (2007).
62. Markus, T. et al. The ice, cloud, and land elevation satellite-2 (ICESat-2): science requirements, concept, and implementation. *Remote Sens. Environ.* https://doi.org/10.1016/j.rse.2016.12.029 (2017).
63. Schwab, M. J. *Reconstruction of the Late Quaternary Climatic and Environmental History of the Schirmacher Oasis and the Wohlthat Massif (East Antarctica)* (Alfred Wegener Institute for Polar and Marine Research, 1998).
64. St-Jean, G. Automated quantitative and isotopic (13C) analysis of dissolved inorganic carbon and dissolved organic carbon in continuous-flow using a total organic carbon analyser. *Rapid Commun. Mass Spectrom.* **17**, 419–428 (2003).
65. St-Jean, G., Kieser, W. E., Crann, C. A. & Murseli, S. Semi-automated equipment for CO_2 purification and graphitization at the A.E. Lalonde AMS Laboratory (Ottawa, Canada). *Radiocarbon* **59**, 941–956 (2017).
66. Crann, C. A. et al. First status report on radiocarbon sample preparation techniques at the A.E. Lalonde AMS Laboratory (Ottawa, Canada). *Radiocarbon* **59**, 695–704 (2017).
67. Kieser, W. E. et al. The André E. Lalonde AMS Laboratory—the new accelerator mass spectrometry facility at the University of Ottawa. *Nucl. Instruments Methods Phys. Res. Sect. B* https://doi.org/10.1016/j.nimb.2015.03.014 (2015).
68. Stuiver, M. & Polach, H. A. Reporting of 14C data. *Radiocarbon* https://doi.org/10.1016/j.forsciint.2010.11.013 (1977).

Acknowledgements

This work was made possible by the Antarctic Logistics Centre International, Cape Town, South Africa, and the Arctic and Antarctic Research Institute/Russian Antarctic Expedition. We are grateful to Colonel (I.L.) J.N. Pritzker, IL ARNG (retired), Lorne Trottier, and fellow field team members for their support during the expeditions. Funding for this research project was provided by the TAWANI Foundation (D. Andersen), the Trottier Family Foundation (D. Andersen), NASA's Exobiology program (D. Andersen), and the Natural Sciences and Engineering Research Council of Canada (D. Lacelle, I.D. Clark & B. Faucher).

Author contributions

B.F., D.L., and D.A. conceived the study; B.F., N.M., D.L., and D.A. acquired data; B.F., N.M., and D.L. developed the numerical modeling; B.F., N.M., D.L., D.A., L.J. and I.C. contributed to drafting; B.F., N.M., D.L., D.A., L.J., and I.C. revised the manuscript; and B.F., N.M., D.L., D.A., L.J., and I.C. approved the submission of the manuscript.

Competing interests

The authors declare no competing interests.

Additional information

Supplementary information The online version contains supplementary material available at https://doi.org/10.1038/s43247-021-00280-x.

Correspondence and requests for materials should be addressed to Benoit Faucher.

Peer review information *Communications Earth & Environment* thanks Jon Telling and the other, anonymous, reviewer(s) for their contribution to the peer review of this work. Primary Handling Editors: Clare Davis. Peer reviewer reports are available.

Reprints and permission information is available at http://www.nature.com/reprints

Publisher's note Springer Nature remains neutral with regard to jurisdictional claims in published maps and institutional affiliations.